ELSEVIER

Journal of Biomechanics 40 (2007) 64–77

JOURNAL OF BIOMECHANICS

www.elsevier.com/locate/jbiomech
www.JBiomech.com

Signaling through the phosphatidylinositol 3-kinase regulates mechanotaxis induced by local low magnetic forces in *Entamoeba histolytica*

C. Rivière[a], S. Marion[b], N. Guillén[b], J.-C. Bacri[a], F. Gazeau[a], C. Wilhelm[a,*]

[a]*Pôle Matière et Systèmes Complexes, Université Paris 7, Denis Diderot, CNRS UMR7057, 140, rue de Lourmel, 75015 Paris, France*
[b]*Unité Biologie Cellulaire du Parasitisme, INSERM U389, Institut Pasteur, 28, rue du Dr Roux 75724, Paris Cedex 15, France*

Accepted 23 November 2005

Abstract

In micro-organisms, as well as in metazoan cells, cellular polarization and directed migration are finely regulated by external stimuli, including mechanical stresses. The mechanisms sustaining the transduction of such external stresses into intracellular biochemical signals remain mainly unknown. Using an external magnetic tip, we generated a magnetic field gradient that allows migration analysis of cells submitted to local low-intensity magnetic forces (50 pN). We applied our system to the amoeba *Entamoeba histolytica*. Indeed, motility and chemotaxis are key activities that allow this parasite to invade and destroy the human tissues during amoebiasis. The magnetic force was applied either inside the cytoplasm or externally at the rear pole of the amoeba. We observed that the application of an intracellular force did not affect cell polarization and migration, whereas the application of the force at the rear pole of the cell induced a persistent polarization and strongly directional motion, almost directly opposed to the magnetic force. This phenomenon was completely abolished when phosphatidylinositol 3-kinase activity was inhibited by wortmanin. This result demonstrated that the applied mechanical stimulus was transduced and amplified into an intracellular biochemical signal, a process that allows such low-intensity force to strongly modify the migration behavior of the cell.

Keywords: Motility; Cell polarization; Mechanotransduction; Cell mechanics

1. Introduction

Cell motility is crucial for many biological processes, such as tissue morphogenesis, leukocyte recruitment to inflammatory sites, angiogenesis, metastasis, and certain parasitic infections. Cell motility is governed by complex interactions between cell surface adhesion molecules, the cytoskeleton, and the extracellular matrix (Kawabata et al., 2001). Basically, crawling cells move in three steps (Serrador et al., 1999). First, the cell becomes polarized through the extension of a leading protrusion. Then, focal adhesion complexes are established at the leading edge, together with de-adhesion at the trailing edge. Finally, contractile forces pull the rear of the cell towards the leading edge. The mechanical forces generated at the leading edge and at the rear of the cell are mainly due to actin filament dynamics and myosin motors activity (Mogilner and Oster, 2003). Cell polarization before movement includes a polarized distribution of organelles, microtubules, and the actin cytoskeleton.

Under many physiological conditions, cell migration is guided by a spatial gradient of soluble compounds that interact with cell surface receptors (Devreotes and Janetopoulos, 2003) to induce attractive (Dormann and Weijer, 2003) or repulsive (Nguyen-Ba-Charvet et al., 2004) directed cell motility in a process called chemotaxis. The binding of the chemoattractant to the surface

*Corresponding author. Tel.: +33 1 44 27 23 16; fax: +33 1 44 27 38 82.
E-mail address: wilhelm@ccr.jussieu.fr (C. Wilhelm).

0021-9290/$ - see front matter © 2005 Elsevier Ltd. All rights reserved.
doi:10.1016/j.jbiomech.2005.11.012

Nomenclature

F_{intra} intracellular magnetic labeling in the presence of the magnetic field gradient = intracellular magnetic force in the 50 pN range

$F_{intra} = 0$ intracellular magnetic labeling in the absence of the magnetic field gradient = No intracellular magnetic force

F_{rear} extracellular magnetic labeling at the rear pole of the cell in the presence of the magnetic field gradient = extracellular magnetic force at the rear pole of the cell in the 50 pN range

$F_{rear} = 0$ extracellular magnetic labeling at the rear pole of the cell in the absence of the magnetic field gradient = No extracellular magnetic force at the rear pole of the cell

Wm Wortmanin

PI3-Kinase phosphatidylinositol 3-kinase

$F_{rear+Wm}$ extracellular magnetic labeling at the rear pole of the cell in the presence of the magnetic field gradient and in the presence of Wortmanin = extracellular magnetic force at the rear pole of the cell in the 50 pN range when PI3-Kinase activity is inhibited.

$F_{rear+Wm} = 0$ extracellular magnetic labeling at the rear pole of the cell in the absence of the magnetic field gradient and in the presence of Wortmanin = No extracellular magnetic force at the rear pole of the cell when PI3-Kinase activity is inhibited

$\langle\ \rangle_i$ average over time (index i)

$\langle V^{inst} \rangle$ average instantaneous velocity (time interval: 1 s)

CME coefficient of movement efficiency, defined as $CME = L/L_t$

L net cell displacement

L_t total distance covered by the cell

$\langle \cos\gamma \rangle = \langle \cos\gamma_i \rangle_i$ the average of cosine γ, the directional angle between the direction of the force and a vector $\overrightarrow{A_0A_i}$, A_0 and A_i being the initial position and each subsequent position, respectively

$\langle \cos\alpha \rangle = \langle \cos\alpha_i \rangle_i$ the average of cosine α, the instantenous directional angle, defined as the directional angle between the direction of the force and a vector $\overrightarrow{A_iA_{i+1}}$, A_i and A_{i+1} being two successive positions of the cell centroid.

$(a_i/b_i)_{inst}$ instantaneous aspect ratio major/minor axis of the equivalent ellipse of the shape of amoebae

$\langle (a/b)_{inst} \rangle = \langle (a_i/b_i)_{inst} \rangle_i$ the average value of the instantaneous aspect ratio major/minor axis calculated at each time interval.

$(a/b)_{mean}$ the mean aspect ratio major/minor axis of the mean cell contour.

receptors triggers a series of cytoplasmic signaling events that notably activate actin filaments polymerization at the leading edge of the cell. The cell senses the direction of the external gradient by spatially regulating the activity of signaling pathways leading to cell polarization, increase in cell speed, and directed movement.

Furthermore, shape changes also occur when adherent cells actively probe the physical properties of the extracellular matrix and build adhesive complexes through their actin-based contractile machinery. Cells integrate such external mechanical stresses through a process called mechanotransduction, which is notably crucial for tissue integrity. The nature and location of the "mechanosensors" at the cell surface, as well as the activity of the contractile actin fibers attached to the cell adhesion sites, are key issues for cell motility.

Various experimental techniques and theoretical models have been developed to unravel the molecular mechanisms involved in cell mechanotransduction. From a theoretical standpoint, several physical models analyzed motile cell as a complex polymer elastic gel submitted to high deformation (Bottino et al., 2002; Gerbal et al., 2000). Experimentally, maps of traction forces generated by the cell have been obtained using deformable substrata with embedded beads (Oliver et al., 1999), a micromachined device consisting of micropatterned cantilevers (Galbraith and Sheetz, 1997) or local indentation with an atomic force microscope (Rotsch et al., 1999). In addition to these "passive" techniques, micromanipulation devices have been developed over a wide force range (1 pN–100 nN), allowing controlled forces to be applied at the cellular or subcellular level and yielding a good description of cellular responses in high stress conditions (Lim et al., 2005). For instance, micromanipulation approaches based on micropipettes aspiration (Usami et al., 1992; Vereycken et al., 1995), cell centrifugation (Koo et al., 2002; Thoumine and Ott, 1997), or shear-flow experiments (Decave et al., 2003; Wojciak-Stothard and Ridley, 2003; Deguchi et al., 2005) have been used to stress the entire cell body. In parallel, by means of functionalized beads (coated with specific ligands), optical and magnetic tweezers give the possibility to apply stresses in well-defined and restricted cell locations (Bausch et al., 1999; Matthews et al., 2004; Schwarzbauer, 1997). Both techniques generate forces in the same range 1–100 pN. The main difference is that in classical optical tweezers set, only one bead at a time can

be controlled. In addition, following cells while they are moving requires sophisticated image analysis and demands feedback to precisely impose the same applied force during the whole experiments length.

Optical and magnetic tweezers techniques have provided new insights on cell mechanical properties (Hu et al., 2004; Puig-de-Morales et al., 2004) and on the interplay between cell adhesion and migration (Galbraith et al., 2002). In particular they allowed a good description of the range of forces generated by the entire cell during adhesion (e.g. few nN; Fukui et al., 2000), but also the level of applied external forces required to modify the activity of the cytoskeleton and transmembrane adhesion compounds. Indeed, forces as low as 0.4–4 pN have been predicted to be sufficient to induce changes in intracellular biochemical signalings (Huang et al., 2004). These findings suggested that cell mechanics cannot be considered as a simple mechanical response of an elastic polymer gel, as it also involves a finely tuned biological signaling response that allows the transduction and amplification of the external stimulus. In particular, external mechanical perturbations have been shown to induce changes in cellular adhesion properties (Bischofs and Schwarz, 2003), and cell motility (Lo et al., 2000).

In experiments using micropipettes (1–30 nN) or microplates (30–200 nN), the applied forces are probably too intense to study such sensitive cell signaling mechanotransduction phenomenon. Therefore, we used in this study low-intensity and well-controlled forces generated by magnetic tweezers (Bausch et al., 1999) to analyze in more details the potential mechanotransduction process involved in cell directional sensing. To this end, we applied forces in the 10–100 pN range to precise locations of the cell, both inside the cytoplasm and externally at the rear pole of polarized migrating cells. The model we chose was the amoeba *E. histolytica*, a parasite causing human amoebic dysentery, which is characterized by an acute tissue invasion and destruction (Stanley, 2003). The invasive trophozoite is a highly motile cell suited to motion analysis (Coudrier et al., 2005). The intracellular organization of *E. histolytica* is simpler than in metazoan cells, because no well-defined endoplasmic reticulum network, and no stable cytoplasmic microtubule network have been yet described (Vayssie et al., 2004). During locomotion, the nucleus and intracellular vesicles are dragged along by cytoplasmic fluxes. The actin cyoskeleton is highly dynamic, enriched in the cortex of the cell and in the frontal pseudopod of polarized trophozoites, within which no actin stress fibers can be observed. Furthermore, *E. histolytica* trophozoites readily engulf human serum-coated magnetic microbeads (Marion et al., 2004), allowing forces to be applied inside the cell cytoplasm. Alternatively, after coating the beads with human IgG, the binding of the beads at the cell surface triggers amoebic IgG-receptors "capping", which induces the clustering of the beads at the rear pole of the cell (Guillen, 1996) and the formation of an appendage called the uropod formed by membrane folding. The latter case allowed us to apply magnetic forces externally at the cell uropod.

In this paper, we investigate the effect of the application of a low-intensity mechanical force on motile *E. histolytica* cells in terms of directional sensing and cell migration. We demonstrated that the application of the force externally at the rear pole of the trophozoites induced a directional sensing phenomenon and the migration of the cells away from the magnetic tip. Interestingly, the cell speed was not increased. We also showed that an active mechanotransduction pathway involving the PI3-Kinase, is necessary to allow such low-intensity force to be amplified inside the cell and thereby to modify cell motility parameters. Therefore, here we established for the first time, an experimental system that allows to precisely study in a physiologic and dynamic manner, the mechanotransduction processes involved in cell directional sensing.

2. Materials and methods

2.1. Cell culture

E. histolytica strain HM1:IMSS was cultured axenically in TYI-S-33 medium (Diamond, 1961) at 37 °C. Pre-incubation of cells with 100 nM Wortmanin (Wm) for 20 min was used to inhibit phosphatidylinositol 3-kinase (PI3-Kinase) activity.

2.2. Magnetic labeling (magnetic beads)

Intracellular magnetic labeling (INTRA experiments) was obtained by incubating *E. histolytica* with 2.8-μm magnetic beads (Dynabeads M-280 tosyl activated; Dynal) coated with total human serum proteins (to activate phagocytosis), for 15 min followed by a period of chase of 3 h at a ratio of 10 beads per amoeba. Amoebas loaded with magnetic beads were placed in the observation chamber.

External magnetic labeling of the cell rear (REAR group) was obtained by triggering *E. histolytica* receptor capping process (Arhets et al., 1995; Calderon and Avila, 1986). Cells were incubated for 10 min with magnetic beads (10 beads/amoeba) covalently coated with human IgG, which stimulate the binding of the beads to specific amoebic IgG-receptors. This triggers receptors capping phenomenon and thereby the irreversible clustering at the beads at the rear pole of the cell.

As shown in Fig. 1, two different groups were studied depending on the localization of the applied force: (F_{intra}, Fig. 1C, and F_{rear}, Fig. 1E). Each group was also

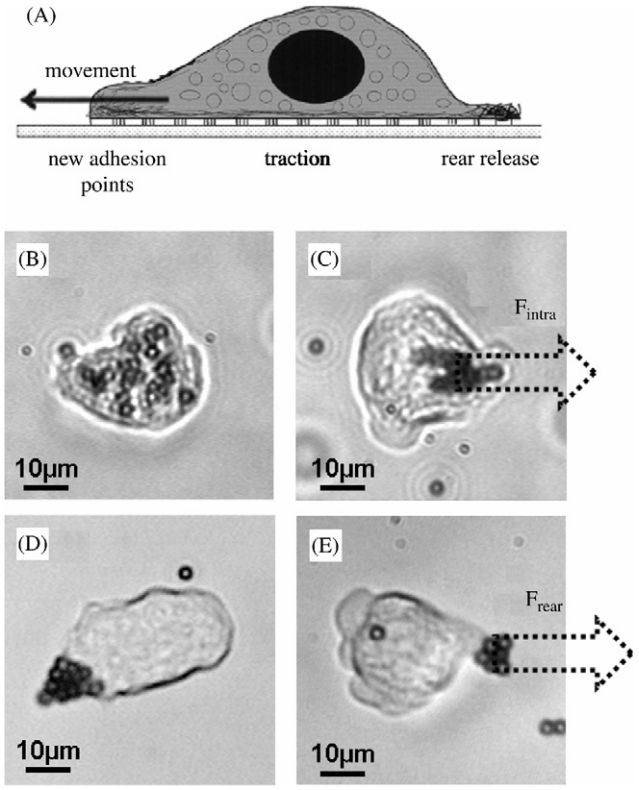

Fig. 1. Magnetic labeling. (A) A schematic view of a polarized amoeba cell, with a pseudopod at the leading edge and a uropod at the rear. (B) Typical intracellular magnetic labeling (2.8-µm magnetic beads) with no applied force ($F_{intra} = 0$) and (C) under force application ($F_{intra} = 50$ pN, dotted arrow). (D) Typical examples of magnetic labeling of the uropod (2.8-µm magnetic beads) with no applied force ($F_{rear} = 0$) and (E) under force application ($F_{rear} = 50$ pN, dotted arrow).

examined in the absence of force application ($F_{intra} = 0$, Fig. 1B and $F_{rear} = 0$, Fig. 1D) e.g. with no external magnetic field applied.

2.3. Incubation chamber and image acquisition

Magnetically labeled amoebas were allowed to adhere for 15 min at 37 °C in a home-made anaerobic glass observation chamber consisting of 2 coverslips separated by a 200-µm-thick plastic spacer and filled with culture medium.

Observations were carried out with an inverted microscope equipped with a 37 °C thermostated platform. Cell motion was recorded with a CCD camera connected to a video-tape recorder. The films were then digitized and processed with NIH software (ScionCorporation, MD, USA) as described below.

2.4. Magnetic force application

A thin magnetic tip, creating a strong magnetic gradient was mounted on a micromanipulator. To precisely calibrate the force experienced by the beads attached to or inside the amoebas, within the chamber (and in the horizontal plane observable through the microscope), we measured the velocity (V_x) of the magnetic beads as they moved towards the magnetic tip in 80% glycerol/20% water (viscosity $\eta = 0.06$ Poiseuille). In the observation window (a 200 µm square), the beads moved with constant velocity and in a direction parallel to the x-axis. The magnetic force F_m was thus precisely counterbalanced by the viscous one:

$$F_D = 3\pi\eta D V_x = F_m, \quad (1)$$

showing that the magnetic force experienced by each bead was 5 pN. This magnetic force is created by the magnetic gradient acting on the superparamagnetic beads: $F_m = m(\text{gradB})_x$, where m is the magnetic moment of the beads. We could thus directly derive the precise magnetic field gradient along the x-axis in the observation window, as follows: $(\text{gradB})_x = 58$ T/m. This gradient is referred below as gradB. About 10 beads are attached to each cell, resulting in a global maximal magnetic force of about 50 pN in both labeling conditions (F_{intra} and F_{rear}). This local force is of the same order as physiological cellular forces such as the ones developed by molecular motors (5 pN) (Ashkin et al., 1990), or the fibronectin/integrin bond strength (30–100 pN) (Lehenkari and Horton, 1999). It is far lower than the integrated traction and contraction forces developed by the cell during migration (nN range) (Galbraith and Sheetz, 1997; Guilford et al., 1995) as well as the adhesion forces concentrated on focal adhesion sites (nN range; Balaban et al., 2001).

2.5. Image analysis

The trajectories and deformations of individual cells during magnetic force application were tracked every 1 s for 500 s, using an in-house NIH image algorithm. Individual amoebas were tracked in each condition: when the force is applied: F_{intra} ($n = 14$), F_{rear} ($n = 14$), $F_{rear+Wm}$ ($n = 12$) and with no force application: $F_{intra} = 0$ ($n = 12$), $F_{rear} = 0$ ($n = 14$), $F_{rear+Wm} = 0$ ($n = 6$). As illustrated in Fig. 2, for each time (index i), the following parameters were recorded:

- the position A_i (x_i,y_i) of the cell centroid,
- the major axis a_i and the minor axis b_i of the "best equivalent ellipse", which approximates the cell shape.

To analyze intracellular bead movements, the instantaneous displacement of the barycenter of the group of beads was tracked (x_i,y_i, origin = centroid). The mean displacement ($\langle \Delta x \rangle$) of this bead barycenter relative to the direction of the applied force was computed for several amoebas.

2.6. Data analysis

For each individual cell, we average over time (index i) instantaneous values, leading to average parameters indicated with brackets ($\langle\ \rangle_i$).

2.6.1. Cell locomotion parameters

Four parameters were used to describe locomotion (Fig. 2A):

- The average instantaneous velocity $\langle V^{inst} \rangle$ (time interval: 1 s).
- The coefficient of movement efficiency (CME), defined as $CME = L/L_t$, where L, the net cell displacement, is the distance, "as the crow flies", covered by the cell during 500 s, and L_t is the total distance covered by the cell, calculated as the sum of the 1-s distances.

CME is a normalized measure of the straightness of the trajectories (Korohoda et al., 1997). CME ranges from 0 (no displacement) to 1 (straight displacement in the same direction).

- The average of cosine γ, $\langle \cos\gamma \rangle = \langle \cos\gamma_i \rangle_i$, where γ_i [0, 360°] is the directional angle between the x-axis (parallel to the force) and a vector $\overrightarrow{A_0A_i}$, A_0 and A_i being the initial position and each subsequent position, respectively. This average cosine describes the global direction of motion (from starting point A_0) and has a value of $+1$ for a cell moving towards the force, -1 for a cell moving away from the force, and 0 for random movement (Djamgoz et al., 2001; Korohoda et al., 1997).
- The average of cosine α, $\langle \cos\alpha \rangle = \langle \cos\alpha_i \rangle_i$, where α_i is the instantaneous directional angle [0, 360°], defined as the directional angle between the x-axis (parallel to the force) and a vector $\overrightarrow{A_iA_{i+1}}$, A_i and

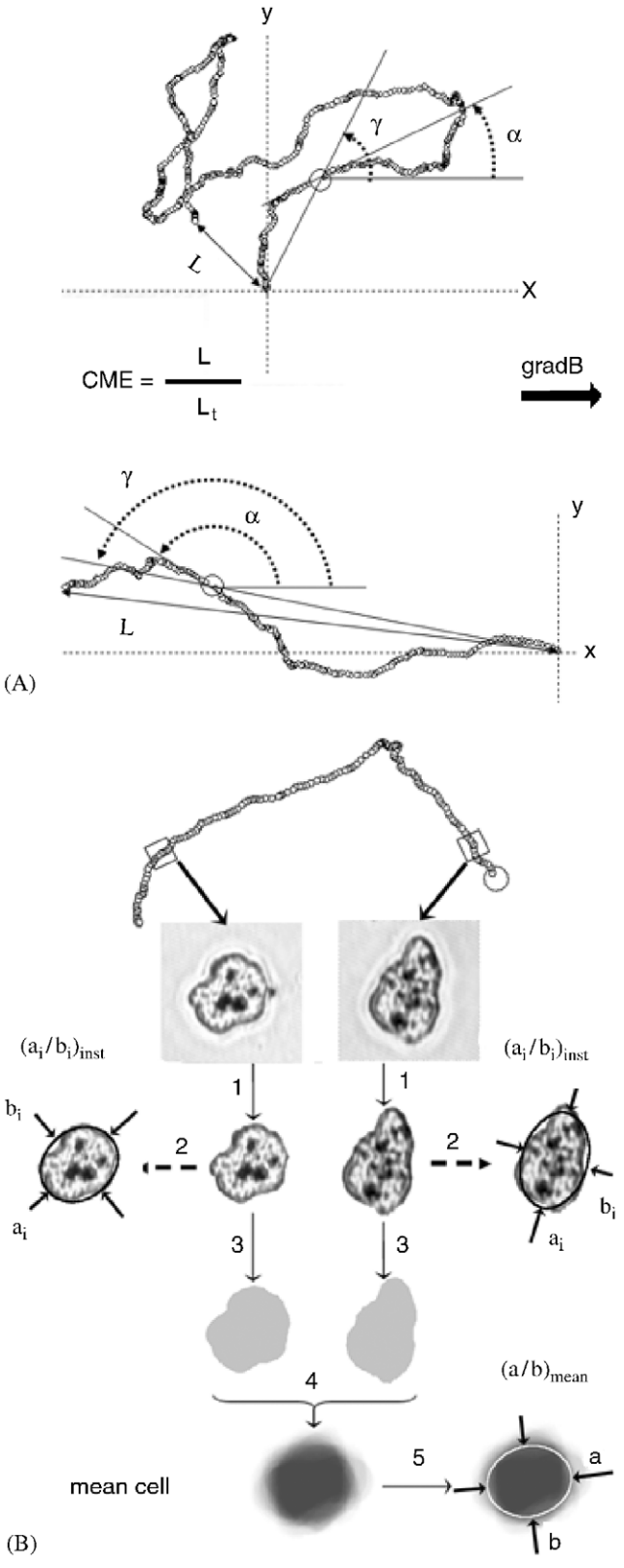

Fig. 2. Locomotion and polarization analysis. Image analysis of amoebic cell migration. The movement of individual cells was tracked every second for 500 s. The images were then analyzed to compute locomotion parameters (A) and polarization parameters (B). (A) Two cell trajectories are represented. For each, the net distance covered by the cell between the first and last point (L) and total length of the cell trajectory (L_t) were calculated. The CME was calculated directly as the ratio between the net displacement L and the total distance L_t covered by the cell. At each point the angles γ and α were computed. Angle γ is the angle between the direction of the force (gradB) and a vector $\overrightarrow{A_0A_i}$, A_0 and A_i being the initial position and each subsequent position, respectively. Angle α is the directional angle between the axis parallel to the force and a vector $\overrightarrow{A_iA_{i+1}}$, A_i and A_{i+1} being two successive positions of the cell centroid. (B) Cell polarization analysis is illustrated for a given cell movement. For each position of the cell, the extracellular medium was cleared (1), the instantaneous aspect ratio $(a_i/b_i)_{inst}$ of the ellipse equivalent was measured (2), the cell cross-sectional surface area was normalized to $\pi(14\,\mu m)^2$ and was filled with gray levels 256/500 (3). The 500 filled surfaces were then fused (4). The center of the mean cell thus obtained is black (gray level 256) and the shades of gray reveal shape fluctuations. The aspect ratio $(a/b)_{mean}$ of the equivalent ellipse (white line) was finally calculated (5).

A_{i+1} being two successive positions of the cell centroid. This average cosine describes the instantaneous direction of the cell and is +1 for a cell moving towards the magnetic gradient, −1 for a cell moving against the magnetic gradient, and 0 for random movement (Djamgoz et al., 2001; Korohoda et al., 1997).

2.6.2. Cell polarization parameters

Image analysis (Fig. 2B) was used to compute polarization parameters for individual amoeba.

First, the external medium was removed (Fig. 2B, stage 1) and the instantaneous aspect ratio $(a_i/b_i)_{\text{inst}}$ of the equivalent ellipse was measured (Fig. 2B, stage 2). The cell surface was then normalized to $a_0 = \pi$ (14 μm^2) and filled with gray level 256/500 (Fig. 2B, stage 3). The 500 filled surfaces were then fused, giving an image of the mean cell shape (Fig. 2B, stage 4). The center of the mean cell thus obtained is black (gray level 256), with decreasing gray values corresponding to changes in cell shape and orientation. This mean shape was used to calculate the mean aspect ratio $(a/b)_{\text{mean}}$ of the equivalent ellipse (Fig. 2B, stage 5).

The polarization of individual amoeba was then described by the two following parameters:

- The average value $\langle (a/b)_{\text{inst}} \rangle = \langle (a_i/b_i)_{\text{inst}} \rangle_i$ of the instantaneous aspect ratio major/minor axis (Fig. 2, stage 2) calculated at each time interval. This parameter is a measure of the cell's instantaneous deformation capacity and is related to pseudopod extensions. The higher the value of $\langle (a/b)_{\text{inst}} \rangle$, the more extended the pseudopods are.
- The mean aspect ratio $(a/b)_{\text{mean}}$, corresponding to the mean cell contour (Fig. 2, stage 5). A sphere has a ratio a/b of 1, while an elongated shape has a ratio larger than 1. This parameter reflects the persistence of the orientation of polarization. Indeed, if the cell extends pseudopods in several directions, the mean cell contour (averaged from the 500 frames) would be close to that of a sphere. In contrast, this value increases when the cell remains polarized in the same orientation; in other words, the higher the $(a/b)_{\text{mean}}$ ratio, the more persistent the orientation of polarization (during the time interval of the experiment: 500 seconds).

2.7. Statistical analysis

Quantitative results in each cell group were expressed as mean ± standard deviation. The significance of the differences between groups was analyzed by performing independent Student's *t*-test between every group (Origin 6.0, Originlab Corporation). Values of $p < 0.001$ were considered significant.

3. Results

The *E. histolytica* trophozoites are highly motile and adherent cells that explore their environment, extending frequently pseudopods in nearly random directions (Coudrier et al., 2005). First we examined whether the magnetic labeling technique consisting on magnetic beads present inside the cytoplasm or bound to the rear pole of the cell induced change in cell motility. To this end, we calculated the polarization and migration parameters of the magnetic labeled amoebas compared to non-labeled ones. We observed that in the absence of the magnetic gradient application, none of the two different magnetic labeling approaches affected cell locomotion or polarization parameters (data not shown). This result demonstrates that the magnetic labeling methods used in this study does not influence random cell motility, a criteria that appeared to us as a crucial prerequisite to study the effect of the magnetic force application on cell migration and polarization.

3.1. Intracellular force application does not affect cell movement

We first applied the magnetic force on motile amoebas that were pre-labeled intracellularly by ingestion of human serum-coated magnetic beads. The amplitude of 50 pN for the applied force was the maximal, reproducible, experimental value we could obtain with our set-up. This force range is far lower than the one used in other micromanipulation techniques such as cell micropipette aspiration, or microplates deformation (in the nN range). Under this condition, we observed that the cells did not migrate up the magnetic gradient generated by the external magnetic tip (Fig. 3). Figs. 3A and B show representative trajectories of two amoebas, in the absence and in the presence of the applied magnetic field, respectively. No qualitative differences were observed. We confirmed this observation by computing the locomotion and polarization parameters for 12 different intracellularly labeled amoebas in control conditions ($F_{\text{intra}} = 0$) and for 14 labeled amoebas submitted to the magnetic field gradient ($F_{\text{intra}} \neq 0$). The CME (Fig. 3C) displayed a value of 0.2 in both conditions, corresponding to a weak cell directionality. Similarly, the near-zero values of both directional parameters $\langle \cos\gamma \rangle$ and $\langle \cos\alpha \rangle$, (Figs. 3D and E, respectively), and the lack of correlation between angles γ and α (Fig. 3F), confirmed the stochastic nature of the trajectories. Therefore, the application of a low-intensity force inside the amoeba cytoplasm did not induce statistical changes in cell motility ($p > 0.001$).

Regarding cell polarization, we examined changes in cell shape calculating the value $(a_i/b_i)_{\text{inst}}$ corresponding to the instantaneous cell shape of one individual amoeba at the instant *i*, and the mean shape of the same amoeba,

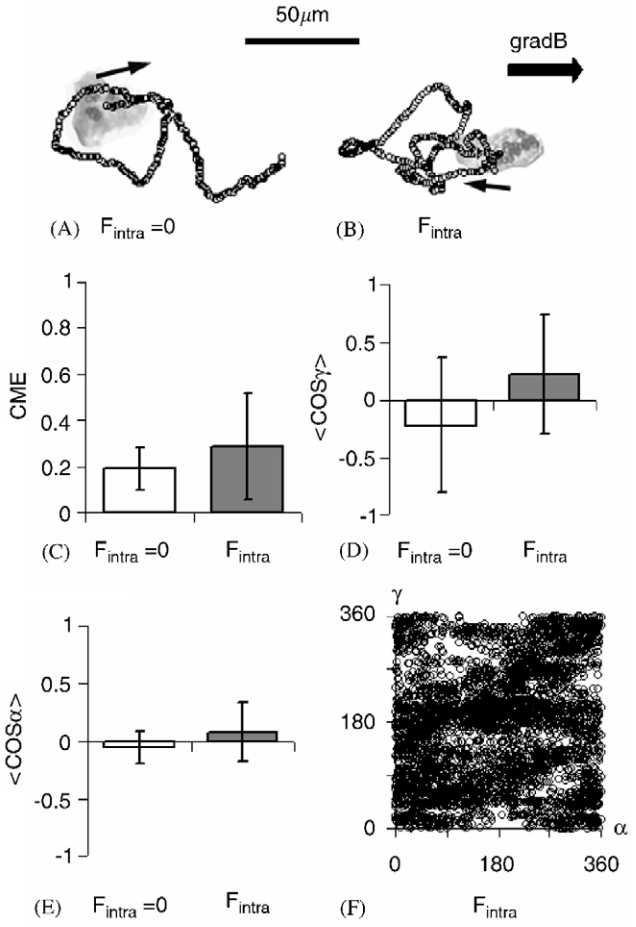

Fig. 3. Intracellular magnetic labeling, locomotion analysis. Examples of cell trajectories for intracellular labeling without an applied force ((A) $F_{intra} = 0$) and under force application ((B) F_{intra}) are given. The direction of the magnetic field gradient (gradB) is indicated. The first image of each corresponding cell is superimposed with the trajectory, indicating the starting position. Arrows indicates initial trajectory direction. (C–E) Mean parameters describing the movement of individual cells under intracellular force application (F_{intra}), with its respective control ($F_{intra} = 0$). Error bars represent amoebas intra-group standard deviation. (C) Mean value for the coefficient of Movement Efficiency (CME). (D) Mean value for $\langle \cos\gamma \rangle$ and (E) Mean value for $\langle \cos\alpha \rangle$. (F) At each point of cell trajectory and for each analyzed cell, the angles (α,γ) are plotted.

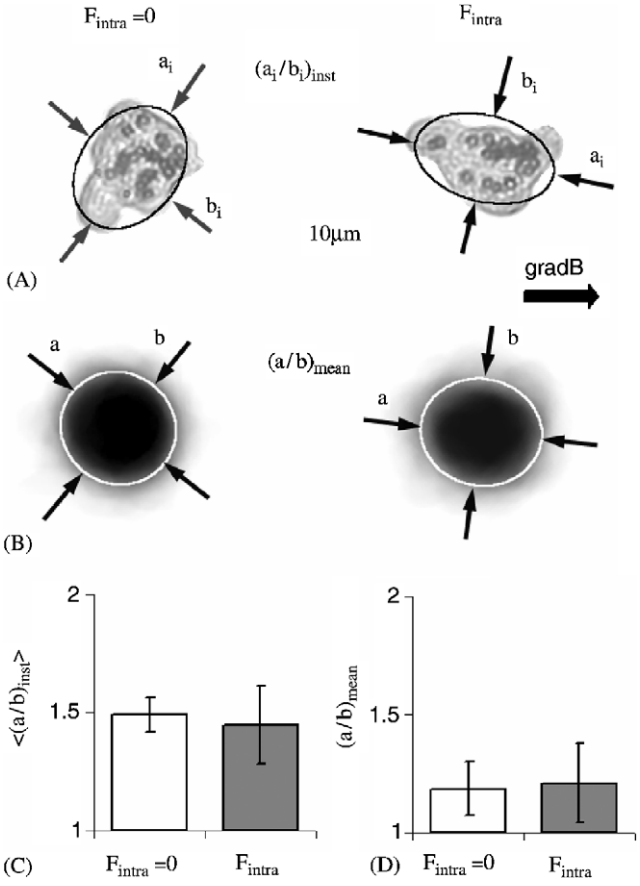

Fig. 4. Intracellular magnetic labeling, polarization analysis. (A) Illustrations of instantaneous polarization analysis of cells at time i (stage 2 in Fig. 2). A typical cell example is given for intracellular labeling without an applied force ($F_{intra} = 0$, left image) and under force application (F_{intra}, right image). $(a_i/b_i)_{inst}$ is calculated from the shape of the cell at each position during tracking (stage 2 in Fig. 2). a_i and b_i being the major and minor axes, respectively. (B) Illustrations of mean polarization analysis of cells $(a/b)_{mean}$, which was obtained by fusing all the instantaneous shapes. A typical cell example is given for intracellular labeling without an applied force ($F_{intra} = 0$, left image) and under force application (F_{intra}, right image). The shape of the equivalent ellipse is superimposed (white line) on the fused mean cell. The corresponding major and minor axes, a and b, give parameter $(a/b)_{mean}$. This parameter gives a measure of the persistence of the orientation of cell polarization. (C–D) Average parameters describing the polarization of individual cells under intracellular force application (F_{intra}), with its respective control ($F_{intra} = 0$). Error bars represent amoebas intra-group standard deviation. (C) Average instantaneous cell polarization $\langle (a/b)_{inst} \rangle$. (B) Mean aspect ratio $(a/b)_{mean}$.

obtained by averaging all the instantaneous shapes during 500 s (Fig. 4A, left : control condition and Fig. 4B, right: amoeba submitted to a magnetic field gradient). For all the amoeba examined within the INTRA group, we did not obtained a significant difference in the degree of instantaneous deformability when the force was applied: $\langle (a/b)_{inst}(F_{intra} \neq 0) \rangle = 1.44 \pm 0.16$ versus $\langle (a/b)_{inst}(F_{intra} = 0) \rangle = 1.49 \pm 0.07$ (Fig. 4C), $p = 0.4$. This indicated that instantaneous deformation (e.g. pseudopod extension) was not affected when the magnetic force is applied inside the cytoplasm of the cell. Similarly, the mean cell deformability value examined over time ($(a/b)_{mean}$) was close to 1 for all the examined amoebas, with no significant difference between the two groups (see Fig. 4B for typical examples and Fig. 4D for the mean values: $(a/b)_{mean}$ $(F_{intra} \neq 0) = 1.20 \pm 0.16$ versus $(a/b)_{mean}$ $(F_{intra} = 0) = 1.18 \pm 0.10$, $p = 0.7$). This value defines that the mean cell shape corresponds to a sphere. This implies that the orientations of the successive extended pseudopods during the 500-s observation period canceled one another out, and that the amoebas therefore showed no persistent polarization in one particular orientation.

To confirm that the intracellular force was indeed operative despite the lack of effect, we tracked the cytoplasmic displacement of the magnetic beads inside several amoebas under application of the magnetic force. The magnetic bead barycenter inside control amoebas showed a diffuse motion and was located close to the cell centroid ($\langle \Delta x \rangle = 0.3 \pm 0.7\,\mu m$). When the magnetic force was applied, this diffuse group of beads moved significantly towards the magnetic source ($\langle \Delta x \rangle = 2.1 \pm 0.5\,\mu m$). Although this deviation did not exceed the bead diameter (2.8 μm), it demonstrated that the force was active inside the cell. This low deviation and the lack of effect on amoeba migration could be partly explained by the fact that the low-intensity applied force (50 pN) is efficiently counterbalanced by mechanical forces generated by cytoplasm fluxes occurring during random movement. The importance of these cytoplasm fluxes was further illustrated by the observation that a doublet of phagosomes can spontaneously be separated inside a motile amoeba. To separate such a pair of magnetic phagosomes, the active force F_{active} acting on each phagosome must overcome the cohesive magnetic dipolar force $F_{dipolar}$. We calculated this force, for magnetic phagosomes submitted to a 0.1-T magnetic field, as

$$F_{active} \geqslant F_{dipolar} = \frac{\mu_0}{4\pi}\frac{6m^2}{d^4} = 63\,pN, \quad (2)$$

where m is the phagosome magnetic moment $m(0.1\,T) = 8 \times 10^{-14}\,A\,m^2$ and $d = 2.8\,\mu m$ is the phagosome diameter. The traction exerted by the external magnetic field, which did not exceed 50 pN, was thus not sufficient to stress the cell and to influence cell movements.

3.2. Extracellular force application at the rear pole induces repulsive mechanotaxis

The incubation of amoebas with human IgG-coated magnetic beads triggers a ''receptor capping'' phenomenon, leading to the adhesion and subsequent clustering of roughly 10 beads per cell at the rear pole of the cell. The application of the magnetic field gradient in these cells markedly modified both cell directionality and polarity. As illustrated in Fig. 5A, amoebas which were not submitted to the magnetic field, displayed stochastic trajectories, confirming that the magnetic labeling of the uropod did not itself perturb cell motility. By contrast, amoebas submitted to the local magnetic force at their rear pole displayed highly directed linear trajectories (Fig. 5B). This effect was quantified by calculating locomotion and polarization parameters (14 cells in each group). When the force was applied, the net displacement of the cell increased nearly three-fold, leading to a marked increase in movement efficiency: CME ($F_{rear} \neq 0$) = 0.77 ± 0.16 versus CME ($F_{rear} = 0$) = 0.3 ± 0.2 (Fig. 5C), $p < 0.001$.

Intriguingly, the calculated parameters average cosine γ and average cosine α displayed both a value close to −1 ($\langle \cos\gamma \rangle = -0.9 \pm 0.1$, $\langle \cos\alpha \rangle = -0.7 \pm 0.1$), demonstrating that the cells moved away from the magnetic source (Figs. 5D and E, respectively). Even if the cells still occasionally changed the direction of their displacement (disparity of α, Fig. 5F), the overall direction remained opposite to the applied force (γ value around 180°, Fig. 5F). Importantly, although the

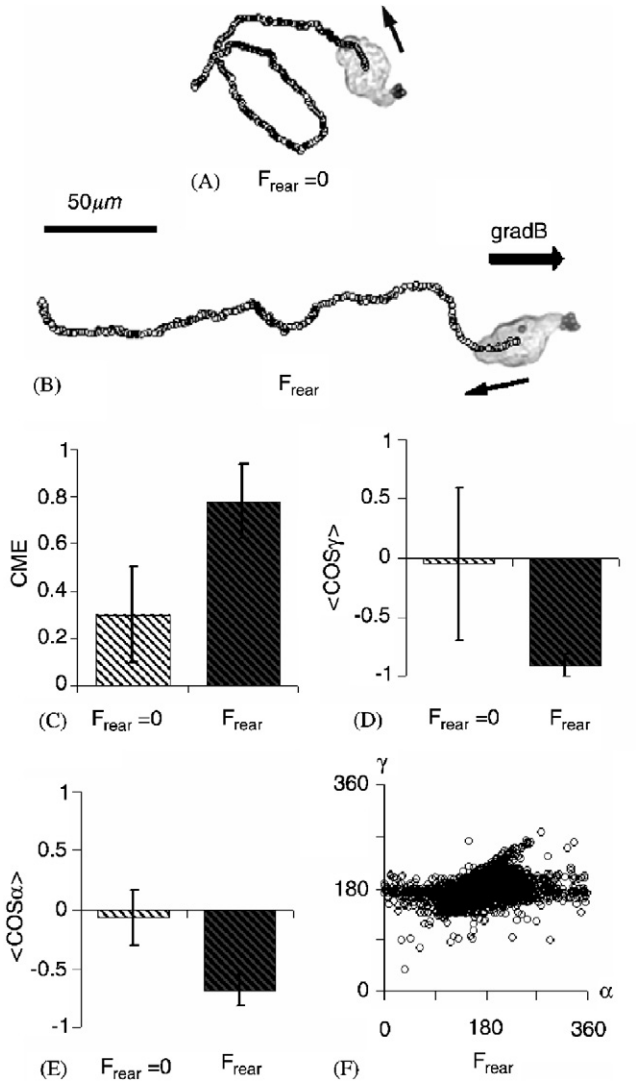

Fig. 5. Extracellular magnetic labeling, locomotion analysis. Examples of cell trajectories for uropod labeling without an applied force ((A) $F_{rear} = 0$) and under force application ((B) F_{rear}) are given. The direction of the magnetic field gradient (gradB) is indicated. The first image of each corresponding cell is superimposed with the trajectory, indicating the starting position. Arrows indicates initial trajectory direction. (C–E) Mean parameters describing the movement of individual cells when force is applied at the rear pole of the cell (F_{rear}), with its respective control ($F_{rear} = 0$). Error bars represent amoebas intra-group standard deviation. (C) Mean value for the coefficient of Movement Efficiency (CME). (D) Mean value for $\langle \cos\gamma \rangle$ and (E) Mean value for $\langle \cos\alpha \rangle$. (F) At each point of cell trajectory and for each analyzed cell, the angles (α,γ) are plotted.

application of the force induced a preferential direction of cell migration, the cell velocity by contrast was not modified: ($\langle V^{\text{inst}}(t=1\,\text{s})(F_{\text{rear}}\neq 0)\rangle = 0.7\pm 0.2\,\mu\text{m/s}$ versus $\langle V^{\text{inst}}(t=1\,\text{s})(F_{\text{rear}}=0)\rangle = 0.6\pm 0.1\,\mu\text{m/s}$, ns).

However, despite the strong observed effect on the direction of cell migration, the application of the force did not modify the instantaneous deformation capacity of the labeled amoeba. Fig. 6A shows the instantaneous shape of one amoeba in the presence and absence of the applied magnetic force. This result was confirmed by calculating the averaged values for 14 different amoeba in the REAR group: $\langle (a/b)_{\text{inst}}(F_{\text{rear}}\neq 0)\rangle = 1.58\pm 0.2$ versus $\langle (a/b)_{\text{inst}}(F_{\text{rear}}=0)\rangle = 1.47\pm 0.14$, ns) (Fig. 6C). By contrast, the mean aspect ratio value, corresponding to the averaged cell shape over the 500 s of observation, was increased after application of the magnetic force at the rear pole of the amoeba: $(a/b)_{\text{mean}}(F_{\text{rear}}\neq 0) = 1.38\pm 0.19$ versus control: $(a/b)_{\text{mean}}(F_{\text{rear}}=0) = 1.17\pm 0.10$ ($p<0.001$, Fig. 6D) (see Fig. 6B for an example of the mean shape of one amoeba tracked during 500 s, in the presence and absence of the applied magnetic force). Upon force application at the cell rear pole, the mean cell shape no longer corresponds to a sphere, as previously observed in the case of random motility, but to an ellipse. Together these results demonstrate that the application of a low-intensity force at the cell uropod induced a preferential direction in the orientation of cell polarization and thereby cell migration. Indeed, one permanent pseudopod was extended in the direction opposite to the magnetic source, without any calculated increase in cell velocity.

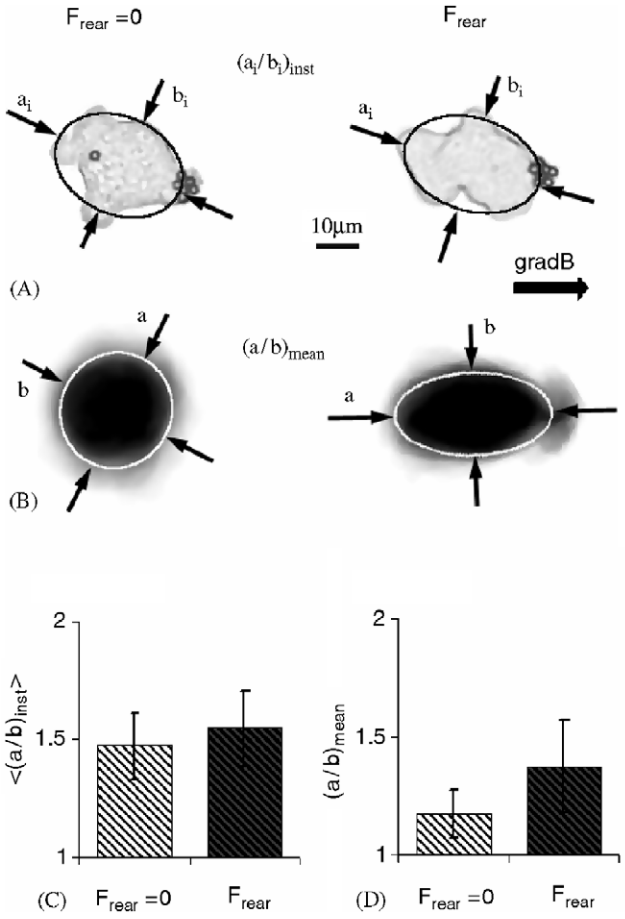

Fig. 6. Extracellular magnetic labeling, polarization analysis. (A) Illustrations of instantaneous polarization analysis of cells at time i (stage 2 in Fig. 2). A typical cell example is given for uropod labeling without an applied force ($F_{\text{rear}}=0$, left image) and under force application (F_{rear}, right image). $(a_i/b_i)_{\text{inst}}$ is calculated from the shape of the cell at each position during tracking. a_i and b_i being the major and minor axes, respectively. (B) Illustrations of mean polarization analysis of cells $(a/b)_{\text{mean}}$, which was obtained by fusing all the instantaneous shapes. A typical cell example is given for intracellular labeling without an applied force ($F_{\text{rear}}=0$, left image) and under force application (F_{rear}, right image). The shape of the equivalent ellipse is superimposed (white line) on the fused mean cell. The corresponding major and minor axes, a and b, give parameter $(a/b)_{\text{mean}}$. This parameter gives a measure of the persistence of the orientation of cell polarization. (C–D) Average parameters describing the polarization of individual cells when the force is applied at the rear pole of the cell (F_{rear}), with its respective control ($F_{\text{rear}}=0$). Error bars represent amoebas intra-group standard deviation. (C) Mean instantaneous cell polarization $\langle (a/b)_{\text{inst}}\rangle$. (B) Mean aspect ratio $(a/b)_{\text{mean}}$.

3.3. *Mechanotransduction of the force applied at the cell rear pole depends on PI3K activity*

In view of this marked cellular response to the weak applied magnetic force, we hypothesized that the mechanical stress was likely transduced and amplified inside the cell into a biological signaling cascade. This signaling cascade would induce the directional sensing phenomenon and thus the observed persistent orientation of the dominant pseudopod (Fig. 6D, $(a/b)_{\text{mean}}$). During chemotactic motility, the PI3-Kinase (PI3K) has been described as a crucial compound for cell directional sensing by translating the external chemical gradient into a steep intracellular gradient resulting in cell polarization (Merlot and Firtel, 2003; Sadhu et al., 2003). We therefore used Wm, a drug that inhibits PI3K activity, to test its potential role in the mechanotaxis phenomenon that we observed when the cells were magnetically labeled at their uropod. The trajectories of 6 amoebas without applied magnetic force, and of 12 amoebas under the application of the magnetic force to their uropod, were tracked after pre-incubation of the cell with Wm.

As shown in Fig. 7, when the magnetic force was applied, the presence of Wm modified the three major locomotion parameters calculated previously in the absence of the drug: CME (Fig. 7A), $\langle \cos\alpha\rangle$ (Fig. 7B) and $\langle \cos\gamma\rangle$ (data not shown). Indeed, the values obtained were similar to the ones calculated for cells that perform random motility (non significant differences). Therefore, in the presence of Wm, the amoebas are not able anymore to sense the external applied mechanical force and to maintain a persistent

directional cell polarization and cell migration. These results demonstrate that a low, local mechanical stress applied to the amoeba is translated inside the cell into a biochemical signal that involved the PI3K activity.

Interestingly, we observed that the presence of Wm did not modify cell polarization during random locomotion observed in the absence of the application of the magnetic force. The instantaneous cell deformability value was comparable to Wm treated cells in the absence of the magnetic force: $\langle (a/b)_{\text{inst}}(F_{\text{rear+Wm}}=0)\rangle = 1.36 \pm 0.27$ and $\langle (a/b)_{\text{inst}}(F_{\text{rear+Wm}}\neq 0)\rangle = 1.36 \pm 0.17$ versus $\langle (a/b)_{\text{inst}}(F_{\text{rear}}\neq 0)\rangle = 1.58 \pm 0.2$ in the absence of Wm (ns, Fig. 7C). This demonstrates that in presence of Wm, the amoeba still exhibited the same migrating behavior as previously observed, extending pseudopods frequently in random directions.

By contrast, Wm abrogated the persistence in the orientation of polarization observed when the magnetic force was applied to the cell rear as the mean aspect ratio $(a/b)_{\text{mean}}$ fell to a value close to 1 (Fig. 7D, $(a/b)_{\text{mean}}(F_{\text{rear+Wm}}\neq 0) = 1.07 \pm 0.03$ compared to $(a/b)_{\text{mean}}(F_{\text{rear}}\neq 0) = 1.38 \pm 0.19$ measured in the absence of Wm, $p<0.001$). This data show that the presence of Wm inhibited the preferential direction of cell polarization induced by a magnetic force applied to the cell rear pole.

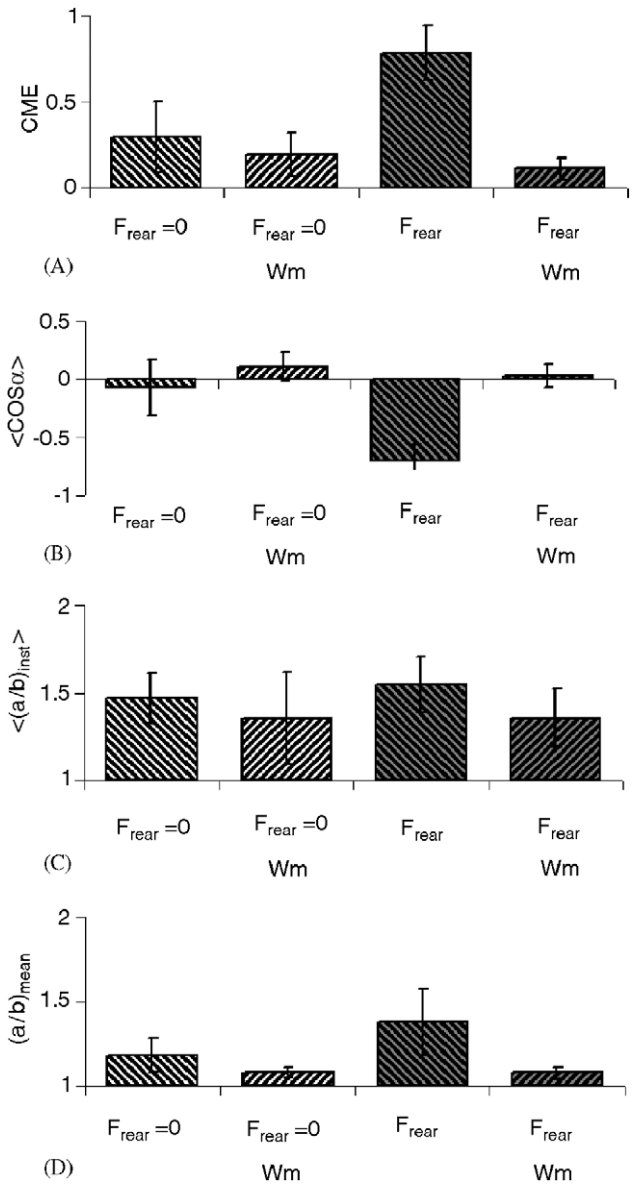

Fig. 7. Extracellular magnetic labeling: locomotion and polarization analysis under the effect of the drug Wortmanin. Comparison of cell movement and cell polarization when the force was applied to the uropod without wortmanin (F_{rear}) and with wortmanin ($F_{\text{rear+Wm}}$), and the respective controls ($F_{\text{rear}}=0$ and $F_{\text{rear+Wm}}=0$). (A, B) Parameters describing directionality (CME (A), and $\langle \cos\alpha \rangle$. (B), as described in Fig. 5). (C, D) Parameters describing polarization (instantaneous aspect ratio $\langle (a/b)_{\text{inst}} \rangle$ (C) and mean aspect ratio $(a/b)_{\text{mean}}$ (D) as described in Fig. 6). Error bars represent amoebas intra-group standard deviation.

4. Discussion

The main purpose of this study was to investigate in the amoeba *E. histolytica*, the cellular polarization and locomotion responses to a weak (50 pN), locally well-defined applied force. By quantitative analysis of cell motility parameters, we found that the magnetic force applied inside the cytoplasm did not affect cell migration, whereas the same force applied externally to the rear pole of the cell induced a persistent orientation of cell polarization and, consequently, a sustained directional displacement resembling chemotaxis.

4.1. Cytoplasmic fluxes overcome intracellular magnetic force: no evidence of intracellular mechanosensing

Theoretical predictions of cell motion have been previously made based on a model of an adhesive elastic gel moving on a solid substrate (Joanny et al., 2003). In this model, the gel polymerizes at the leading front and depolymerizes at the rear. The motion results then from the competition between a self-generated swelling gradient and the adhesion to the substrate. This model predicts that the effect of an external force applied on the moving gel depends on where precisely the force is applied. Inside the adherent gel, representing the cytoplasm of a living cell, no effect occurs until the applied force is sufficient to break the adhesive links between the gel and the substrate. In our assay, the exogenous magnetic force that we applied inside the cell is low (about 50 pN) and had no detectable effect on cell motility or cell polarization. Notably, the force is three orders of magnitude weaker than intracellular forces generated by contractile mechanisms involved in cellular adhesion (1–20 nN) (Tan et al., 2003). Those cellular adhesion forces are governed mainly through focal adhesion sites, where transmembrane protein complexes

"sense" the physical properties of the local external environment (Bershadsky et al., 2003; Chen et al., 2004; Nicolas et al., 2004; Wozniak et al., 2004). This theoretical model can partly explain our findings. Indeed, the force that we applied inside the cell appears too low to break cellular adhesion links with the substrate and thereby should not have any effect on the migration of *E. histolytica*.

An alternative explanation could be that the low magnetic force we applied is efficiently counterbalanced by the forces generated by cytoplasm fluxes during amoeba random migration. This hypothesis is emphasized by the observation of the spontaneous disruption of phagosome pairs during cell movement. In conclusion, although we demonstrated that the intracellular magnetic force we applied inside the cell was effective, it did not trigger any effect on amoeba migration. Moreover, even if extracellular mechanical forces have been previously shown to trigger intracellular signaling cascades, to our knowledge, there is no evidence of intracellular mechanosensing phenomenon. This is also our finding with our intracellular magnetic force.

4.2. Mechanorepelent effect after the application of an extracellular force

By contrast, we observed marked changes in *E. histolytica* migration when the magnetic force was applied externally to the rear pole of the cell. The amoeba exhibited a persistent polarization and a strongly directional movement away from the magnetic source.

By opposition to the case when the force is applied inside the gel, the theoretical model of (Joanny et al., 2003) predicts that if the external force is applied to the rear of the gel and particularly opposing the direction of gel motion, it should increase the actin filament depolymerization rate and thus increase the gel velocity, creating a so called "negative" motility. In a similar way, part of the results regarding the induction of directed motion of *Dictyostelium discoideum* under shear-flow have also been interpreted by a physical model where the plasma membrane suffers a "peeling process" above a force threshold application related to cell adhesion forces (Garrivier et al., 2002). Our experimental findings could be partly explained by these physical models, because we also found that *E. histolytica* response to the application of a magnetic force strongly depended on where the force was applied, and was effective only after application at the rear pole of the cell.

However, the force applied in our experiments (50 pN) is far lower than the integrated force developed by the migrating cells, which are in the nanoNewton range (Galbraith and Sheetz, 1997). Other evidence of such high-intensity force generated by the cell during migration is given by the observation of cells capable to move over long distances against a flow applying forces in the 10–100 pN range (Decave et al., 2003). Therefore, we hypothesized that the "negative" effect of the force on the direction of amoeba migration cannot be explained without a mechanism where the external mechanical stimulus is transduced and amplified into an intracellular biochemical signal, which in turn stimulates a persistent cell polarization.

4.3. Extracellular mechanosensing of low force intensity (50 pN) at the rear pole of the cell: implication of PI3K

We focused our analysis on the implication of the PI3-Kinase in the potential mechanostransduction phenomenon as this compound has been shown to play a fundamental role in directional sensing and cell polarization (Devreotes and Janetopoulos, 2003) from the amoeba *D. discoideum* to the neutrophils (Servant et al., 2000) or fibroblasts (Haugh et al., 2000).

During chemotaxis, the local amount of PIP3, synthesized by PI3K, has indeed been reported to be the first signaling agent creating a steep intracellular gradient allowing F-actin polymerization to be activated locally at the pole of the cell facing the chemoattractant gradient. PI3K has also been shown to play an essential role to maintain the direction of cell migration, e.g. the persistence of polarization, towards the external gradient in *D. discoideum* and in leukocytes (Sadhu et al., 2003). Therefore, PI3K and its lipid product PIP3 appear to be the cell's compass that identify and determine the orientation of cell asymmetry that create directed movement (Rickert et al., 2000; Weiner, 2002). Furthermore, the evidence that PI3K activity is involved in mechanotransduction has also been highlighted in shear-flow studies on *D. discoideum* (Decave et al., 2003) and on endothelial cells (Urbich et al., 2002). Its role in cardiovascular physiology, where mechanical deformation is a key issue, and in related diseases, has also been reported (see Oudit et al., 2004, for a review).

We therefore tracked the migration of *E. histolytica* trophozoites labeled with magnetic beads at their rear pole in the presence of Wm a well-known compound that inhibits PI3K activity. We observed that Wm completely inhibited both the persistent polarization and directed movement in response to the applied magnetic force. The cells still move as if no force were applied, exploring the surrounding environment extending pseudopods in random directions. Therefore, the sensing of the external magnetic force was completely abolished. This data demonstrated that PI3K is crucial for the intracellular transduction of the external mechanical stimulus. The initial mechanosensors as well as the signaling pathway involved in this PI3K-mediated mechanotransduction are still unknown. Nevertheless, our experimental system appears as a unique tool to

investigate upstream effectors of the PI3K involved in the observed directional sensing as well as in the molecular mechanisms involved in the persistence of pseudopod extension.

4.4. Mechanotaxis: distinctions between directional sensing and cell migration

During chemotaxis, the chemo-attractant receptors are uniformly localized around the cells. Preferential receptor occupancy at the pole of the cell facing the gradient triggers locally the activation and amplification of signaling pathways involved in directional sensing and cell polarization. First, directional sensing of the gradient is mediated by activation of PI3K that allows the creation of a steep intracellular gradient of PIP3. Directional sensing of the external stimulus is followed by cell polarization characterized by the local activation of F-actin nucleation at the pole of the cell facing the gradient. This results in an increase in cell speed. This pathway involved key molecules such as the Rho-family GTPases that relay the signal to the cytoskeleton, through the Wasp/Scar-Arp2/3 pathway activation. Several feedbacks loops are then involved to amplify and maintain the local Rho-GTPase activation and subsequent membrane protrusion at one pole of the cell (see Merlot and Firtel, 2003; Van Haastert and Devreotes, 2004, for a review). More importantly, directional sensing, defined by the re-localization of PI3K, is a process independent of cell polarization, as it was shown that the cell is able to sense the external chemoattractant gradient even in the presence of drugs that inhibit F-actin polymerization.

During chemotaxis, changes in the instantaneous cell shape can be used as a read-out for the activity of the actin polymerization dynamics. Indeed, for motile cells such as the amoeba *D. discoideum*, which extend spontaneously frequent pseudopods without activation by an external stimulus, the presence of a chemoattractant gradient induces the formation of longer and persistent pseudopods, together with an increase in cell speed.

Surprisingly, in our mechanotaxis assay, the external magnetic force induced drastic changes in direction of migration, without any increase in cell velocity, or changes in instantaneous cell shape. Therefore, as proposed both for mechanotaxis (Decave et al., 2003) and chemotaxis (Hannigan et al., 2002) studies, cell speed, determined by the F-actin polymerization/depolymerization rates and direction of migration appeared in this study controlled by independent mechanisms.

Noteworthy, to our knowledge, all previous studies preformed on mechanotaxis involved the application of high-intensity mechanical stimuli inducing changes in cell polarization always combined with an increase in cell speed. Therefore, our approach is the first described method that can allow uncoupling these two phenomena and studying more accurately in a dynamic manner the early sensing step and the molecular mechanisms involved in the maintenance of cell polarization.

We can conclude that the magnetic force application acts as a compass leading to pseudopod extension in a unique direction. The persistent pseudopod formed is oriented in the direction precisely opposite to the applied force, while the formation of secondary pseudopods is completely inhibited on lateral sides of the cell. This observation is similar to what was found during chemotaxis in other cells where PTEN, the phosphatase responsible for PIP3 dephosphorylation, is localized to the lateral sides of the cell and inhibits pseudopod extension. It would be now interesting to localize PTEN and PI3K during the mechanotransduction assay to investigate if the molecular mechanosensing mechanisms are similar or different from the ones involved in chemical sensing.

The system we developed in this study could offer the possibility to discover new detailed insights into the physical and biochemical processes involved in cell migration in vitro and can be correlated to the in vivo complex cell migration behaviour. Related to *E. histolytica*, it was shown that chemotaxis is involved in the switch to virulence of the parasite and is crucial for human tissue invasion. Therefore, by using mutant strains and drug treatments, the system developed in this study would allow to gain insights into the virulent factors involved in amoebiasis.

Acknowledgments

This work was supported by the Ministère de l'Education Nationale de l'Enseignement Supérieur et de la Recherche (ACI nanosciences, nanotechnologie), and the French Direction Générale de l'Armement (DGA).

References

Arhets, P., Gounon, P., Sansonetti, P., Guillen, N., 1995. Myosin II is involved in capping and uroid formation in the human pathogen *Entamoeba histolytica*. Infection and Immunity 63, 4358–4367.

Ashkin, A., Schutze, K., Dziedzic, J.M., Euteneuer, U., Schliwa, M., 1990. Force generation of organelle transport measured in vivo by an infrared laser trap. Nature 348, 346–348.

Balaban, N.Q., Schwarz, U.S., Riveline, D., Goichberg, P., Tzur, G., Sabanay, I., Mahalu, D., Safran, S., Bershadsky, A., Addadi, L., Geiger, B., 2001. Force and focal adhesion assembly: a close relationship studied using elastic micropatterned substrates. Nature Cell Biology 3, 466–472.

Bausch, A.R., Moller, W., Sackmann, E., 1999. Measurement of local viscoelasticity and forces in living cells by magnetic tweezers. Biophysical Journal 76, 573–579.

Bershadsky, A.D., Balaban, N.Q., Geiger, B., 2003. Adhesion-dependent cell mechanosensitivity. Annual Review of Cell and Developmental Biology 19, 677–695.

Bischofs, I.B., Schwarz, U.S., 2003. Cell organization in soft media due to active mechanosensing. Proceedings of the National Academy of Sciences 100, 9274–9279.

Bottino, D., Mogilner, A., Roberts, T., Stewart, M., Oster, G., 2002. How nematode sperm crawl. Journal of Cell Sciences 115, 367–384.

Calderon, J., Avila, E.E., 1986. Antibody-induced caps in *Entamoeba histolytica*: isolation and electrophoretic analysis. The Journal of Infectious Diseases 153, 927–932.

Chen, C.S., Tan, J., Tien, J., 2004. Mechanotransduction at cell–matrix and cell–cell contacts. Annual Review of Biomedical Engineering 6, 275–302.

Coudrier, E., Amblard, F., Zimmer, C., Roux, P., Olivo-Marin, J.C., Rigothier, M.C., Guillen, N., 2005. Myosin II and the Gal-GalNAc lectin play a crucial role in tissue invasion by *Entamoeba histolytica*. Cellular Microbiology 7, 19–27.

Decave, E., Rieu, D., Dalous, J., Fache, S., Brechet, Y., Fourcade, B., Satre, M., Bruckert, F., 2003. Shear flow-induced motility of *Dictyostelium discoideum* cells on solid substrate. Journal of Cell Sciences 116, 4331–4343.

Deguchi, S., Maeda, K., Ohashi, T., Sato, M., 2005. Flow-induced hardening of endothelial nucleus as an intracellular stress-bearing organelle. Journal of Biomechanics 38, 1751–1759.

Devreotes, P., Janetopoulos, C., 2003. Eukaryotic chemotaxis: distinctions between directional sensing and polarization. Journal of Biological Chemistry 278, 20445–20448.

Diamond, L.S., 1961. Axenic cultivation of *Entamoeba histolytica*. Science 134, 336–337.

Djamgoz, M.B.A., Mycielska, M., Madeja, Z., Fraser, S.P., Korohoda, W., 2001. Directional movement of rat prostate cancer cells in direct-current electric field: involvement of voltagegated Na+ channel activity. Journal of Cell Sciences 114, 2697–2705.

Dormann, D., Weijer, C.J., 2003. Chemotactic cell movement during development. Current Opinion in Genetics & Development 13, 358–364.

Fukui, Y., Uyeda, T.Q., Kitayama, C., Inoue, S., 2000. How well can an amoeba climb? Proceedings of the National Academy of Sciences 97, 10020–10025.

Galbraith, C.G., Sheetz, M.P., 1997. A micromachined device provides a new bend on fibroblast traction forces. Proceedings of the National Academy of Sciences 94, 9114–9118.

Galbraith, C.G., Yamada, K.M., Sheetz, M.P., 2002. The relationship between force and focal complex development. The Journal of Cell Biology 159, 695–705.

Garrivier, D., Decave, E., Brechet, Y., Bruckert, F., Fourcade, B., 2002. Peeling model for cell detachment. European Physics Journal E: Soft Matter 8, 79–97.

Gerbal, F., Chaikin, P., Rabin, Y., Prost, J., 2000. An elastic analysis of *Listeria monocytogenes* propulsion. Biophysical Journal 79, 2259–2275.

Guilford, W.H., Lantz, R.C., Gore, R.W., 1995. Locomotive forces produced by single leukocytes in vivo and in vitro. American Journal of Physiology 268, C1308–C1312.

Guillen, N., 1996. Role of signalling and cytoskeletal rearrangements in the pathogenesis of *Entamoeba histolytica*. Trends in Microbiology 4, 191–197.

Hannigan, M., Zhan, L., Li, Z., Ai, Y., Wu, D., Huang, C.K., 2002. Neutrophils lacking phosphoinositide 3-kinase gamma show loss of directionality during *N*-formyl-Met-Leu-Phe-induced chemotaxis. Proceedings of the National Academy of Sciences 99, 3603–3608.

Haugh, J.M., Codazzi, F., Teruel, M., Meyer, T., 2000. Spatial sensing in fibroblasts mediated by 3′ phosphoinositides. The Journal of Cell Biology 151, 1269–1280.

Hu, S., Eberhard, L., Chen, J., Love, J.C., Butler, J.P., Fredberg, J.J., Whitesides, G.M., Wang, N., 2004. Mechanical anisotropy of adherent cells probed by a three-dimensional magnetic twisting device. American Journal of Physiology—Cell Physiology 287, C1184–C1191.

Huang, H., Kamm, R.D., Lee, R.T., 2004. Cell mechanics and mechanotransduction: pathways, probes, and physiology. American Journal of Physiology—Cell Physiology 287, C1–C11.

Joanny, J.-F., Jülicher, F., Prost, J., 2003. Motion of an adhesive gel in a swelling gradient: a mechanism for cell locomotion. Physical Review Letter 90, 168102.

Kawabata, K., Nagayama, M., Haga, H., Sambongi, T., 2001. Mechanical effects on collective phenomena of biological systems: cell locomotion. Current Applied Physics 1, 66–71.

Koo, L.Y., Irvine, D.J., Mayes, A.M., Lauffenburger, D.A., Griffith, L.G., 2002. Co-regulation of cell adhesion by nanoscale RGD organization and mechanical stimulus. Journal of Cell Sciences 115, 1423–1433.

Korohoda, W., Golda, J., Sroka, J., Wojnarowicz, A., Jochym, P., Madeja, Z., 1997. Chemotaxis of *Amoeba proteus* in the developing pH gradient within a pocket-like chamber studied with the computer assisted method. Cell Motility and the Cytoskeleton 38, 38–53.

Lehenkari, P.P., Horton, M.A., 1999. Single integrin molecule adhesion forces in intact cells measured by atomic force microscopy. Biochemical and Biophysical Research Communications 259, 645–650.

Lim, C.T., Zhou, E.H., Quek, S.T., 2006. Mechanical models for living cells–a review. Journal of Biomechanics 39, 195–216.

Lo, C.M., Wang, H.B., Dembo, M., Wang, Y.L., 2000. Cell movement is guided by the rigidity of the substrate. Biophysical Journal 79, 144–152.

Marion, S., Tavares, P., Arhets, P., Guillen, N., 2004. Signal transduction through the Gal-GalNAc lectin of *Entamoeba histolytica* involves a spectrin-like protein. Molecular and Biochemical Parasitology 135, 31–38.

Matthews, B.D., Overby, D.R., Alenghat, F.J., Karavitis, J., Numaguchi, Y., Allen, P.G., Ingber, D.E., 2004. Mechanical properties of individual focal adhesions probed with a magnetic microneedle. Biochemical and Biophysical Research Communications 313, 758–764.

Merlot, S., Firtel, R.A., 2003. Leading the way: directional sensing through phosphatidylinositol 3-kinase and other signaling pathways. Journal of Cell Sciences 116, 3471–3478.

Mogilner, A., Oster, G., 2003. Polymer motors: pushing out the front and pulling up the back. Current Biology 13, R721–R733.

Nguyen-Ba-Charvet, K.T., Picard-Riera, N., Tessier-Lavigne, M., Baron-Van Evercooren, A., Sotelo, C., Chedotal, A., 2004. Multiple roles for slits in the control of cell migration in the rostral migratory stream. The Journal of Neuroscience 24, 1497–1506.

Nicolas, A., Geiger, B., Safran, S.A., 2004. Cell mechanosensitivity controls the anisotropy of focal adhesions. Proceedings of the National Academy of Sciences 101, 12520–12525.

Oliver, T., Dembo, M., Jacobson, K., 1999. Separation of propulsive and adhesive traction stresses in locomoting keratocytes. The Journal of Cell Biology 145 (3), 589–604.

Oudit, G.Y., Sun, H., Kerfant, B.G., Crackower, M.A., Penninger, J.M., Backx, P.H., 2004. The role of phosphoinositide-3 kinase and PTEN in cardiovascular physiology and disease. Journal of Molecular and Cellular Cardiology 37, 449–471.

Puig-de-Morales, M., Millet, E., Fabry, B., Navajas, D., Wang, N., Butler, J.P., Fredberg, J.J., 2004. Cytoskeletal mechanics in adherent human airway smooth muscle cells: probe specificity and scaling of protein–protein dynamics. American Journal of Physiology—Cell Physiology 287, C643–C654.

Rickert, P., Weiner, O.D., Wang, F., Bourne, H.R., Servant, G., 2000. Leukocytes navigate by compass: roles of PI3Kgamma and its lipid products. Trends in Cell Biology 10, 466–473.

Rotsch, C., Jacobson, K., Radmacher, M., 1999. Dimensional and mechanical dynamics of active and stable edges in motile

fibroblasts investigated by using atomic force microscopy. Proceedings of the National Academy of Sciences 96, 921–926.
Sadhu, C., Masinovsky, B., Dick, K., Sowell, C.G., Staunton, D.E., 2003. Essential role of phosphoinositide 3-kinase delta in neutrophil directional movement. The Journal of Immunology 170, 2647–2654.
Schwarzbauer, J.E., 1997. Cell migration: may the force be with you. Current Biology 7, R292–R294.
Serrador, J.M., Nieto, M., Sanchez-Madrid, F., 1999. Cytoskeletal rearrangement during migration and activation of T lymphocytes. Trends in Cell Biology 9, 228–233.
Servant, G., Weiner, O.D., Herzmark, P., Balla, T., Sedat, J.W., Bourne, H.R., 2000. Polarization of chemoattractant receptor signaling during neutrophil chemotaxis. Science 287, 1037–1040.
Stanley Jr., S.L., 2003. Amoebiasis. Lancet 361, 1025–1034.
Tan, J.L., Tien, J., Pirone, D.M., Gray, D.S., Bhadriraju, K., Chen, C.S., 2003. Cells lying on a bed of microneedles: an approach to isolate mechanical force. Proceedings of the National Academy of Sciences 100, 1484–1489.
Thoumine, O., Ott, A., 1997. Comparison of the mechanical properties of normal and transformed fibroblasts. Biorheology 34, 309–326.
Urbich, C., Dernbach, E., Reissner, A., Vasa, M., Zeiher, A.M., Dimmeler, S., 2002. Shear stress-induced endothelial cell migration involves integrin signaling via the fibronectin receptor subunits alpha(5) and beta(1). Arteriosclerosis, Thrombosis, and Vascular Biology 22, 69–75.
Usami, S., Wung, S.L., Skierczynski, B.A., Skalak, R., Chien, S., 1992. Locomotion forces generated by a polymorphonuclear leukocyte. Biophysical Journal 63, 1663–1666.
Van Haastert, P.J., Devreotes, P.N., 2004. Chemotaxis: signalling the way forward. Nature Review Molecular Cellular Biology 5, 626–634.
Vayssie, L., Vargas, M., Weber, C., Guillen, N., 2004. Double-stranded RNA mediates homology-dependent gene silencing of gamma-tubulin in the human parasite *Entamoeba histolytica*. Molecular and Biochemical Parasitology 138, 21–28.
Vereycken, V., Bucherer, C., Lacombe, C., Lelievre, J.C., 1995. [A study of leukocyte chemotaxis in a glass micropipette]. Journal des Maladies Vasculaires 20, 113–116.
Weiner, O.D., 2002. Regulation of cell polarity during eukaryotic chemotaxis: the chemotactic compass. Current Opinion in Cell Biology 14, 196–202.
Wojciak-Stothard, B., Ridley, A.J., 2003. Shear stress-induced endothelial cell polarization is mediated by Rho and Rac but not Cdc42 or PI 3-kinases. The Journal of Cell Biology 161, 429–439.
Wozniak, M.A., Modzelewska, K., Kwong, L., Keely, P.J., 2004. Focal adhesion regulation of cell behavior. Biochimica et Biophysica Acta 1692, 103–119.